図 5. 粉砕に φ 0.05 mm のジルコニアボールを用いた Ni-Alfa および NiO-Sigma の
10%FBS-MEM 懸濁液の調製後（左）および 37℃で 1 日静置後（右）の粒径分布
（上：散乱強度分布、下：個数分布）

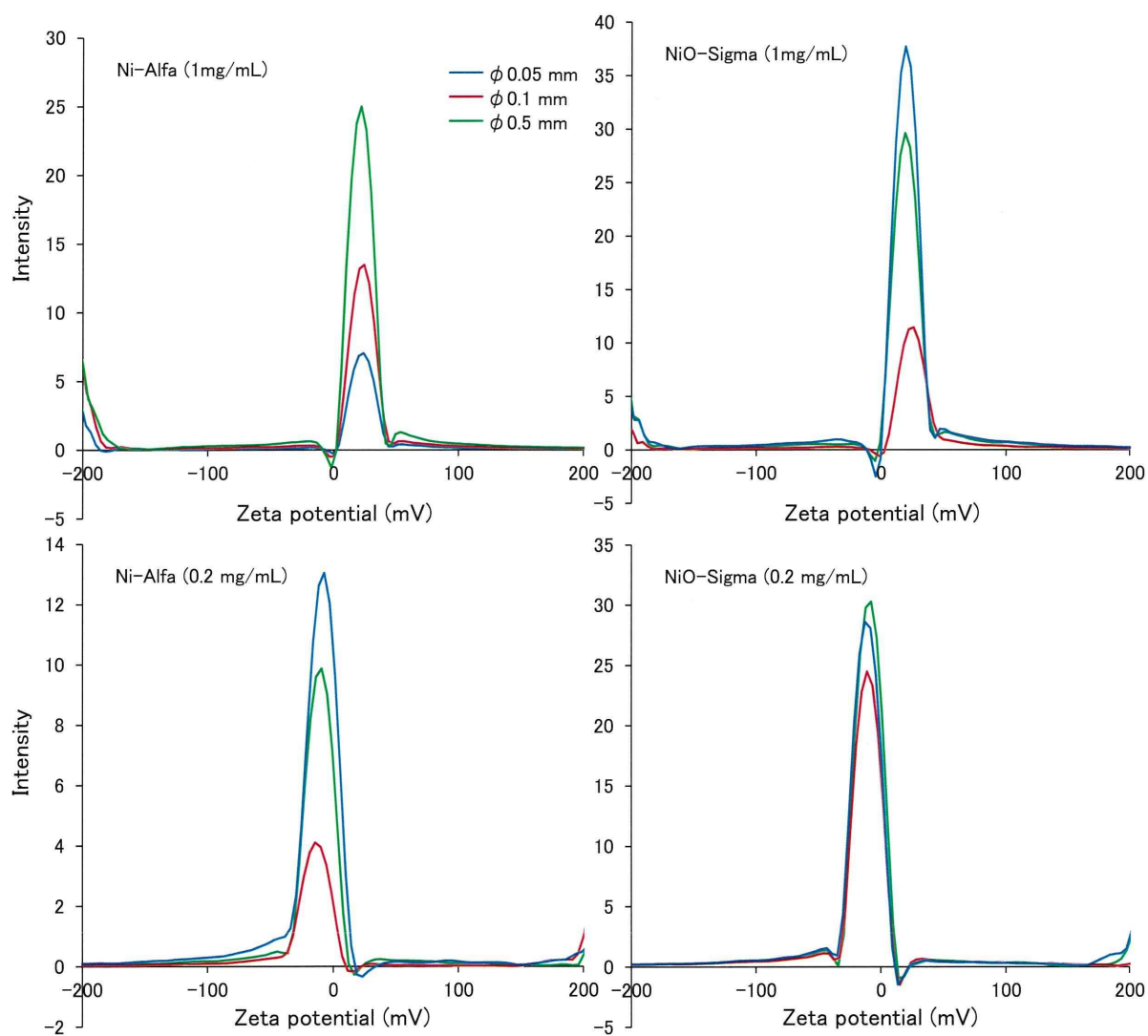図 6. Ni-Alfa および NiO-Sigma の懸濁原液および 10%FBS-MEM 懸濁液の Zata 電位

III. 研究成果の刊行に関する一覧表

研究成果の刊行に関する一覧表

書籍

著者氏名	論文タイトル名	書籍全体の編者名	書籍名	出版社名	出版地	出版年	ページ
D. Kami, M. Toyoda, M. Watanabe, S. Gojo.	Pleiotropic functions of magnetic nanoparticles for ex vivo gene transfer and cell transplantation therapy.	Jitendra Naik	Nano Based Drug Delivery.	IAPC-OBP	Croatia	2015	547-55

雑誌

発表者氏名	論文タイトル名	発表誌名	巻号	ページ	出版年
A. Iwasaki, K. Sakai, K. Moriya, T. Sasaki, D. R. Keene, M. Watanabe, S. Morishita, T. Sakai.	Molecular mechanism responsible for fibronectin-controlled alterations in tissue stiffness in advanced chronic liver fibrogenesis.	J. Biol. Chem.	291 (1)	72-88	2016
T. Kondo, K. Mori, M. Hachisu, T. Yamazaki, D. Okamoto, M. Watanabe, K. Gonda, H. Tada, Y. Hamada, M. Takano, N. Ohuchi, Y. Ichiyanagi.	AC magnetic susceptibility and heat dissipation by Mnl-xZnxFe2O4 nanoparticles for hyperthermia treatment.	J. Appl. Phys.	117	17D157	2015

Y. Ito, H. Ishiguro, N. Kobayashi, H. Hasumi, M. Watanabe, M. Yao, H. Uemura.	Adipocyte-derived monocyte chemotactic protein-1 (MCP-1) promotes prostate cancer progression through the induction of MMP-2 activity.	Prostate	75(10)	1009-19	2015
K. Hayashi, W. Sakamoto, T. Yogo.	Smart ferrofluid with quick gel transformation in tumors for MRI-guided local magnetic thermochemotherapy.	Adv. Funct. Mater.	26(11)	1708-18	2016
K. Ishino, T. Kato, M. Kato, T. Shibata, M. Watanabe, K. Wakabayashi, H. Nakagama, Y. Tostuka.	Comprehensive DNA aauct analysis reveals pulmonary inflammation response contributes to genotoxic action of magnetic nanoparticles.	Int. Mol. Sci.	16 (2)	3474-92	2015
M. Komiya, G. Fujii, S. Miyamoto, M. Takahashi, R. Ishigamori, W. Onuma, K. Ishino, Y. Tostuka, K. Fujimoto, M. Mutoh.	Suppressive effects of the NADPH oxidase inhibitor apocynin on intestinal tumorigenesis in obese KK-Ay and Apc mutant Min mice.	Cancer Sci.	106 (11)	1499-505	2015
N. Hanagata, H. Morita.	Calcium ions rescue human lung epithelial cells from the toxicity of zinc oxide nanoparticles.	J. Toxicol. Sci.	40 (5)	625-35	2015

L. Xu, M. Dan, A. Shao, X. Cheng, C. Zhang, R. A. Yokel, T. Takemura, N. Hanagata.	Silver nanoparticles induce tight junction disruption and astrocyte neurotoxicity in a rat blood-brain barrier primary triple coculture model.	Int. J. Nanomed.	10	6105-18.	2015
岩﨑有由美, 岡本大樹, 遠藤宣弘, 渡邉昌俊.	前立腺癌治療へのナノ粒子の応用	医学のあゆみ	252(4)	303-8	2015

IV. 研究成果の刊行物・別刷

Molecular mechanism responsible for fibronectin-controlled alterations in tissue stiffness in advanced chronic liver fibrogenesis

Ayumi Iwasaki[1,7#], Keiko Sakai[1,2#], Kei Moriya[2#], Takako Sasaki[3], Douglas R. Keene[4], Riaz Akhtar[5], Takayoshi Miyazono[6], Satoshi Yasumura[6], Masatoshi Watanabe[7], Shin Morishita[8], and Takao Sakai[1,2]

[1]MRC Centre for Drug Safety Science, Department of Molecular and Clinical Pharmacology, Institute of Translational Medicine, University of Liverpool, Liverpool L69 3GE, UK;
[2]Department of Biomedical Engineering, Lerner Research Institute, Cleveland Clinic, Cleveland, OH 44195, USA;
[3]Department of Biochemistry, Faculty of Medicine, Oita University, Oita, 879-5593, Japan;
[4]Micro-Imaging Center, Shriners Hospital for Children, Portland, OR 97231, USA;
[5]Centre for Materials and Structures, School of Engineering, University of Liverpool, Liverpool L69 3GH, UK;
[6]Department of Gastroenterology and Hepatology, and Transfusion Medicine and Cell Therapy, Toyama University, Toyama 930-0194, Japan;
Graduate School of [7]Biomedical Engineering and [8]Environmental and Information Science, Yokohama National University, Yokohama 240-8501, Japan.

#These authors contributed equally to this work

Running title: Tissue stiffness in advanced liver fibrosis

Key Words: extracellular matrix; fibronectin; tissue stiffness; lysyl oxidase; TGF-β; chronic hepatic fibrogenesis; mouse model of liver disease; conditional knockout mouse

Correspondence: Takao Sakai, M.D., Ph.D., MRC Centre for Drug Safety Science, Department of Molecular and Clinical Pharmacology, Institute of Translational Medicine, University of Liverpool, Sherrington Building, Ashton Street, Liverpool L69 3GE, United Kingdom.
TEL: 0151-795-2704; FAX: 0151-794-5540; Email: sakait@liverpool.ac.uk

Abstract

Fibrosis is characterized by extracellular matrix (ECM) remodeling and stiffening. However, the functional contribution of tissue stiffening to non-cancer pathogenesis remains largely unknown. Fibronectin (Fn) is an ECM glycoprotein substantially expressed during tissue repair. Here we show in advanced chronic liver fibrogenesis using a mouse model lacking Fn that, unexpectedly, Fn-null livers lead to more extensive liver cirrhosis, which is accompanied by increased liver tissue stiffness and deteriorated hepatic functions. Furthermore, Fn-null livers exhibit more myofibroblast phenotypes, and accumulate highly disorganized/diffuse collagenous ECM networks composed of thinner and significantly increased number of collagen fibrils during advanced chronic liver damage. Mechanistically, mutant livers show elevated local TGF-β activity and lysyl oxidase expressions. A significant amount of active lysyl oxidase is released in Fn-null hepatic stellate cells in response to TGF-β1 through canonical and non-canonical Smad such as PI3 kinase-mediated pathways. TGF-β1-induced collagen fibril stiffness in Fn-null hepatic stellate cells is significantly higher compared to wild-type cells. Inhibition of lysyl oxidase significantly reduces collagen fibril stiffness, and treatment of Fn recovers collagen fibril stiffness to wild-type levels. Thus, our findings indicate an indispensable role for Fn in chronic liver fibrosis/cirrhosis in negatively regulating TGF-β bioavailability, which in turn modulates ECM remodeling and stiffening, and consequently preserves adult organ functions. Furthermore, this regulatory mechanism by Fn could be translated for a potential therapeutic target in broader variety of chronic fibrotic diseases.

Introduction

Fibrosis is a part of the wound-healing response that maintains organ structure and integrity following tissue damage. However excessive fibrosis contributes to a number of diseases such as liver

63

fibrosis (1). Liver fibrosis is defined as an abnormal response of the liver to persistent injury and affects tens of millions of people worldwide (2). It is caused by hepatotropic virus infection, drug and alcohol abuse. Liver fibrosis is of great clinical importance since normal liver architecture is disrupted and liver function is ultimately impaired. There is no effective treatment for liver fibrosis and many patients end up with a progressive form of the disease, liver cirrhosis, often requiring a liver transplant (3,4). The hallmark of liver fibrosis is excessive accumulation of mainly type I collagen-containing extracellular matrices (ECMs), and therefore involves both wound healing and fibrotic processes. ECM production and remodeling in the liver following injury involves the activation of specific cell types, hepatic stellate cells, which transdifferentiate into contractile and proliferative myofibroblasts (5-7).

Collagen is the most abundant scaffolding ECM in tissue/organ stroma and contributes significantly to tissue/organ integrity (8). The Lysyl oxidase (LOX) family enzymes are copper-dependent amine oxidases that catalyze the process of covalent crosslinking of collagen by oxidatively deaminating specific lysine and hydroxylysine residues in the telopeptide domains, which increases collagen stiffness (9,10). Collagen crosslinking stiffens the ECM and has been implicated in cancer cell invasion (11). Collagen crosslinking also accompanies tissue fibrosis mediated by several profibrogenic cytokines (12). However, the functional contribution of collagen crosslinking to non-cancer pathogenesis remains largely unknown.

Transforming growth factor (TGF)-β is a profibrogenic master cytokine responsible for promoting differentiation of tissue-resident fibroblasts into myofibroblasts, upregulation of ECM production including fibronectin (Fn), and downregulation of ECM degradation (13). Growing evidence suggests a mechanism by which Fn plays a role in TGF-β signaling (14). Fn is involved in the initial incorporation of latent TGF-β-binding protein (LTBP)-1 into the ECM *in vitro* (15). TGF-β is secreted in a biologically inactive (latent) form in a complex (large latent complex [LLC]) with TGF-β latency associated protein (LAP) and LTBPs (16). The extracellular TGF-β activity in response to injury is regulated by the local activation of latent TGF-β complex to active TGF-β. Indeed, elevated TGF-β bioavailability is frequently observed in chronic fibrotic diseases, and the inhibition of local TGF-β activation can protect against the progression of fibrosis in several adult chronic fibrotic diseases (17-20). In spite of numerous *in vitro* studies and

animal models, TGF-β/Fn interdependence in the fibrogenic response to advanced chronic liver damage has not yet been addressed *in vivo*.

Fn is a large dimeric glycoprotein that exists in blood plasma in its soluble form (plasma type) and in its insoluble form (cellular type) as a part of the ECM of almost every tissue in an organism. Plasma Fn is produced solely by hepatocytes in the liver (21,22). Extensive *in vitro* functional studies have indicated that Fn plays a key role in a wide range of cellular behaviors (21,22), and prominent expression of Fn is observed in response to liver injury (23). Based on *in vitro* findings, it has been postulated that collagen network formation depends on the Fn matrix (24,25). We therefore hypothesized that removal of Fn from the *in vivo* system could prevent extensive ECM network formation following tissue damage. To define the functional identity of Fn in adult tissue remodeling, we recently established a null-condition for both Fn isoforms in adult liver. We demonstrated a Fn-independent mechanism of collagen fibrillogenesis and identified TGF-β-signaling and type V collagen as essential elements for collagen fibrillogenesis in response to liver injury (26). However, it remains unknown whether the extent of the initial Fn deposition could contribute to the critical turning point from normal to abnormal healing during the development of chronic tissue fibrosis. Furthermore, it is also unclear how ECM remodeling by myofibroblasts results in changes in mechanical tension and supports the activation of pathogenic signaling pathways. Here, we have addressed the molecular mechanism responsible for tissue stiffness in advanced chronic liver fibrogenesis using a mouse model lacking both Fn isoforms in the adult liver.

Experimental Procedures

Maintenance of mice
Mice lacking both plasma and cellular type fibronectin in the liver (liver Fn-null mice) were generated by intraperitoneal injections of polyinosinic-polycytidic acid (pI-pC) in the Fn(fl/fl)/*Mx-Cre*+ strain as described previously (26). Fn-null livers showed normal liver morphology, and no obvious inflammation or fibrosis was noted after pI-pC injections (26). All mice were maintained and bred at the animal facility in the Cleveland Clinic, OH, USA, and the University of Liverpool, Liverpool, UK, in accordance with institutional guidelines. Mice were regularly

monitored and had free access to standard mouse chow and water. Mice received humane care in accordance with institutional guidelines.

Induction of chronic liver injury by carbon tetrachloride (CCl₄)

Chronic liver injury was induced intraperitoneally by administrations of CCl_4 solution in olive oil (Fluka) (0.5 ml/kg body weight as 50% [vol/vol], twice a week for up to 17 weeks) in sex-matched, 12- to 15-week-old mice (26,27). Control and liver Fn-null mice were derived from the same litters. Mice injected only with olive oil as negative controls showed no phenotypes (data not shown).

Antibodies, cytokines and reagents

The following antibodies were used for the analyses: rabbit polyclonal antibody (pAb) against mouse fibronectin (Chemicon); rabbit mAb (E184, Epitomics) against αSMA; rabbit pAb against pSmad3 which specifically recognizes the phosphorylated C-terminal serine 423/425 of Smad3 (also cross-reacted with phosphorylated C-terminal serine 465/467 of Smad2) (a kind gift from Dr. Koichi Matsuzaki, Kansai Medical University, Osaka, Japan); rabbit pAb against LOX (Sigma-Aldrich); rabbit pAb against cleaved caspase3 (Cell Signaling); mouse mAb against HSC70 (Santa Cruz); mouse mAb against β-actin (clone AC15, Sigma); affinity-purified rabbit pAbs against mouse LAP of TGF-β1, mouse LTBP-3, human LTBP-4, and human type V collagen (26). The preparation and characterization of rabbit pAbs against bovine type I collagen and type III procollagen have been described elsewhere (28). Rabbit pAb against human lysyl oxidase was generated using its protein residue #22-168 expressed in HEK293 cells as an antigen and affinity purified as described (29). Rabbit pAb against LTBP-1 was a kind gift from Dr. Lynn Sakai (Research Center, Shriners Hospitals for Children, Portland, OR, USA). FITC- and Cy3-conjugated donkey anti-rabbit IgG, and peroxidase-conjugated donkey anti-mouse and anti-rabbit IgG were from Jackson ImmunoRes Lab. 4'6-diamidino-2-phenylindole (DAPI) was from Molecular Probes. Envision™+ System-HRP labeled polymer was from DAKO. Recombinant human TGF-β1 was from R&D Systems. Bovine plasma fibronectin was from Sigma. All inhibitors were from Calbiochem.

Histological analysis, immunohistochemistry and immunofluorescence, and transmission electron microscopy

For histological analysis, liver samples were either directly frozen in OCT compound (Tissue-Tek, Sakura Finetek) or fixed overnight in 4% paraformaldehyde in PBS, pH 7.2, and dehydrated in a graded alcohol series before being embedded in paraffin. Sirius Red staining was performed according to standard protocols. Immunohistochemistry and immunofluorescence studies were performed as described previously (30,31). Double-immunohistochemical analysis with paraffin-embedded tissue sections was performed as described (26). Briefly, after the first antigen-antibody reaction, the slides were incubated with dissociation buffer containing 0.1 M Glycine-HCl (pH 2.2) to dissociate immunoglobulins from antigenic sites. Then the second antigen-antibody reaction was subsequently performed. We carried out the second reaction without antibodies and confirmed the complete dissociation of the first immunoglobulins.

For quantification of fibrotic areas in response to chronic liver injury and LOX signal intensity in hepatic stellate cells, images were captured with the same gain, offset, magnitude and exposure time. A minimum of 5 different images were randomly selected, and intensities were quantified using ImageJ software (version 1.48, US National Institutes of Health). For cellular signal intensity, the mean intensity in each cell (intensities/areas, 50 cells) was measured and the average intensity per cell (relative fluorescent units) was calculated as described elsewhere (32).

Transmission electron microscopy (TEM) was performed as described previously (26).

Polarization microscopy analysis

Quantitative polarization microscopic analysis was performed on Sirius red stained sections using Abrio™ LS PolScope (CRI Inc., Woburn, MA) (33). In PolScope images, the brightness of each pixel is strictly proportional to birefringence "retardance" of the particular object point and independent of its slow axis orientation (34). Measured retardances and orientations are represented as pseudo-colors. Images make it possible to determine specimen anisotropy (retardance and azimuth) at all angles (360°) simultaneously, and permit quantitative measurements on the orientation and the degree of organization of the fibers (35). In the present analysis, any azimuth (slow axis orientation) was covered by a 180° range because a fiber bundle has no head or tail. Fiber retardations and orientations were assessed with an automated analyzing system. Fifty measurements were taken in each of the three

65

regions and averaged. The degree of fiber alignment is represented by a calculation of the angular deviation of each orientation distribution. Thus, the smaller the angular deviation, the more aligned the fibers are.

Atomic force microscopy (AFM) analysis

The nanomechanical properties of the liver sections were investigated with atomic force microscopy (AFM: NanoScope VIII MultiMode AFM, Bruker Nano Inc., Santa Barbara, CA). The AFM was equipped with a $150 \times 150 \times 5$ μm scanner (J-scanner) operated with the Peakforce Quantitative Nanomechanical Mapping (PFQNM) modality. Liver samples were rapidly frozen in OCT compound (Tissue-Tek, Sakura Finetek) following which 10 μm thick sections were prepared using a cryostat (Leica CM1950, Leica Microsystems, UK) and adhered to glass slides coated with Vectabond (Vector Laboratories Ltd). Cells were directly seeded on glass coverslips and cultured for 7 days. Then the glass slides/cover slips were adhered to metal support stubs using adhesive pads, and the samples were imaged at ambient conditions using a silicon nitride tip. The tip had a nominal tip radius of 8 nm and a 5 N/m spring constant (Bruker TAP150A probe). The preparation method used for the AFM imaging maintained the tissue/cellular structure for imaging without the need for any chemical fixation. The PFQNM method was calibrated using a reference polymer (PS1, Vishay Measurements Group UK) with a known elastic modulus (2.8 ± 0.1 GPa). The spring constant and deflection sensitivity was calibrated using the reference sample and the same AFM probe was used for imaging every sample. The data were fitted with the Derjaguin–Muller–Toporov (DMT) model to extract the elastic modulus, as described previously (36). For tissue samples, 10 x 10 μm images were collected and the mean elastic modulus was determined using Bruker Nanoscope software, v 1.5. Each image had a resolution of 384 samples/line. The regions selected for AFM were guided by Sirius Red-stained images of serial sections. Smaller scans (2 x 2 μm) were conducted in collagen fibril-rich areas and used to determine the elastic modulus distribution pixel-by-pixel in these locations. A Gaussian fit was applied to the data. For cell culture samples, collagen fibril areas were selected from 5 x 5 μm scan images, and the mean elastic modulus for collagen fibrils were determined from 0.5 x 0.5 μm scans.

Real-time PCR

Real-time PCR was performed as described previously (37). The following primers were used:

Col1a1 forward, 5'-GGGCGAGTGCTGTGCTTT-3';
Col1a1 reverse, 5'-GGTCCCTCGACTCCTACATCTTC-3';
Col3a1 forward, 5'-CTGTAACATGGAAACTGGGGAAA-3';
Col3a1 reverse, 5'-CCATAGCTGAACTGAAAACCACC-3';
Col5a1 forward, 5'-GAGGACCACACAGGGAAGC-3';
Col5a1 reverse, 5'-CTTGTAGACACTGAGAGCAATTCG-3';
MMP8 forward, 5'-GGGATTATGGAAATGCCTCGAT-3';
MMP8 reverse, 5'-CTGTTTTCACTTCAGCCCTTGA-3';
MMP13 forward, 5'-CTTCTTCTTGTTGAGCTGGACTC-3';
MMP13 reverse, 5'-CTGTGGAGGTCACTGTAGACT-3';
LOX forward, 5'-CCTATGCGGCAGACATAGACT-3';
LOX reverse, 5'-CCAGGTAGCTGGGGTTTACA-3';
LOXL1 forward, 5'-ATGTGCAGCCTGGGAACTAC-3';
LOXL1 reverse, 5'-CACCACGTTGTTGGTGAAGT-3';
LOXL2 forward, 5'-CGTTGGAGTGGTGTGTAGTGAG-3';
LOXL2 reverse, 5'-CGAAAGGCAGAAAGGATGG-3';
LOXL3 forward, 5'-GCCACGTAGTCTGCGGTATG-3';
LOXL3 reverse, 5'-AGGGAGAGGTGGGCTTCTGT-3';
LOXL4 forward, 5'-GCCGCTGCAAGTATGATGG-3';
LOXL4 reverse, 5'-CCTGAGTCGCTGTTCCTGCT-3';
18S rRNA forward, 5'-GGCGACGACCCATTCG-3';
18S rRNA reverse, 5'-ACCCGTGGTCACCATGGTA-3'.

All samples were analyzed in triplicate as a minimum. After the reactions, the specificity of amplifications in each sample was confirmed by dissociation analysis, showing that each sample gave a single melting peak. The relative mRNA levels were normalized to the level of *18S rRNA*.

Western-blot analysis

Western blot analyses were performed as described elsewhere (31). In some immunoblotting analyses, samples were transferred onto an Immobilon-FL polyvinylidene fluoride (PVDF) membrane (Millipore Corp.) and probed with primary and IRDye 800CW- or IRDye 680-conjugated secondary antibodies (LI-COR Biosci.). Immunoreactive bands were detected using the Odyssey Infrared Imaging System (LI-COR Biosci.).

TGF-β bioassay

A mink lung cell line (TMLC) stably transfected with a plasminogen activator inhibitor-1 (PAI-1) promoter fused to luciferase was used for the analysis (38). Active TGF-β levels were measured as described elsewhere (32).

Hydroxyproline assay

Hydroxyproline content was measured as described elsewhere (26).

Hepatic biochemical markers

Serum alanine aminotransferase (ALT) level was determined using a standard kit (Genzyme Diagnostics P.E.I. Inc., Canada). Serum total protein (by the Biuret method), albumin (by the BCG method), total bilirubin (by the Azobilirubin method), and cholinesterase (by the p-Hydroxybenzolcholine method) levels were measured using the Hitachi 7180 Auto Analyzer (Japan).

In vitro assay using mouse hepatic stellate cell lines

Control and Fn-null mouse hepatic stellate cell lines were established from adult primary hepatic stellate cell cultures under p21-null genetic background as described previously (26) and used for the analysis presented in this study. Briefly, hepatic stellate cells were isolated from adult Fn(flox/flox)/p21(-/-) mouse liver as parental cells, and subsequently those lines were treated with *Cre*-transducing adenovirus to delete *Fn-floxed genes* (Fn-null hepatic stellate cells). Established cell lines showed similar morphology and typical activated hepatic stellate cell phenotypes (26). To examine the effects of TGF-β1 on LOX production, hepatic stellate cells were cultured for 8 h with Dulbecco's modified Eagle's medium (DMEM) containing 8 % Fn-depleted FBS. The medium was then replaced with DMEM without FBS containing 0.2 mM ascorbic acid and 2 pM TGF-β1. Cells were then incubated for 18 h and used for the analysis. To examine the

inhibitory effect of collagen crosslinking, cells were treated with β-aminopropionitrile (BAPN, 200 μM: Fisher Scientific) containing DMEM, 8 % Fn-depleted FBS, 0.2 mM ascorbic acid and 2 pM TGF-β1, then incubated for 7 days and used for the analysis. We confirmed that the concentration of BAPN used did not affect stellate cell proliferation (data not shown). To examine the effect of Fn on formed collagen stiffness, cells were cultured for 7 days with DMEM containing 8 % Fn-depleted FBS, 0.2 mM ascorbic acid and 10 μg/ml plasma Fn, then used for the analysis. To examine the signaling axis in TGF-β1-mediated LOX production, Fn-null stellate cells were cultured for 24 h with DMEM containing 8 % Fn-depleted FBS. The medium was then replaced with DMEM containing 0.2 mM ascorbic acid without FBS and with indicated supplements. Cells were preincubated for 1 hr, then treated with 2 pM TGF-β1, further incubated for 18 h, then analyzed. Where indicated, cultures contained 10 μM SIS3 (IC_{50}=3 μM) to inhibit Smad3, 10 μM LY294002 (IC_{50}=1.4 μM) to inhibit phosphatidylinositol 3 (PI3)-kinase, 10 μM PD169316 (IC_{50}=89 nM) to inhibit p38 MAP kinase, 5 μM 420119 (IC_{50}=40 nM) to inhibit c-Jun N-terminal kinase (JNK), and 20 μM PD98059 (IC_{50}=2 μM) to inhibit mitogen-activated protein kinase kinase (MEK)1/2. We confirmed that the concentration of the inhibitors used did not affect stellate cell proliferation (data not shown).

Data presentation and statistical analysis

All experiments were performed in triplicate as a minimum, on separate occasions, and the data shown were chosen as representative of results consistently observed. Results are presented as means ± standard deviation (S.D.). Differences between selected groups were analyzed using the Mann-Whitney *U* test. In cases where more than two groups were compared, the Steel-Dwass test was used. A *P* value of <0.05 was considered significant.

Results

More extensive fibrosis/cirrhosis in mice lacking Fn during CCl₄-induced advanced stages of chronic liver injury.

Based on our previous finding that Fn-deficiency did not interfere with reconstruction and resolution of collagen organization in initial stages of liver damage (26), we hypothesized that Fn-deficiency

may not affect the reconstruction of ECM architectures even in advanced stages of chronic liver damage. To address functional roles of Fn during this process, chronic liver fibrosis was induced in a well-established mouse model where injury is brought on by treatment with a liver-damaging agent, carbon tetrachloride (CCl_4, 0.5 ml/kg weight, twice a week for 17 weeks) (27). While increased expression of Fn protein was observed in control livers after injury, its expression in mutant livers (Fn(fl/fl)/Mx-Cre+) was remarkably low throughout the experimental period (time 0 through 17 weeks during CCl_4 injections). The Fn level in mutant livers at 17 weeks of CCl_4 treatment was only ~2% of that in control livers ($P < 0.01$) as shown by Western analysis (Fig. 1A; and data not shown). These data confirmed that neither Fn isoform was induced in mutant livers during advanced chronic injury. Anatomical and histological analyses revealed no abnormalities in Fn-null livers under standard laboratory conditions ((26), data not shown).

To determine whether Fn-deficiency affects CCl_4-induced liver damage during chronic injury, body weight changes, serum alanine aminotransferase (ALT, as a measure for hepatocyte damage) and albumin/globulin ratio (as a measure of net hepatic damage) were examined. These parameters showed similar patterns in both control and Fn-null livers during 17 weeks of CCl_4 treatment. Both showed no increase in body weight and a gradual decrease of ALT activity from 4 to 17 weeks and albumin/globulin ratio from 0 to 17 weeks (Fig. 1B, C), confirming the advanced stages of chronic liver injury in both control and mutant livers (39). Fibrosis was then assessed by Sirius Red staining, which allows visualization of collagen fibers. Histologically, both control and mutant livers developed complete fibrosis patterns throughout the regions such as the P-C bridge (between the portal area and the central vein) and C-C bridge formations (between the central veins) (Fig. 1D), indicating micronodular cirrhosis (27). Unexpectedly, Fn-null livers developed more extended and significant fibrosis. Approximately 12% of the livers were Sirius Red positive, representing a 3.2-fold increase over control livers (Fig. 1D, $P < 0.01$). Taken together, these findings indicate that prolonged and persistent chronic damage caused by 17 weeks of CCl_4 treatment does establish advanced liver fibrosis/micronodular cirrhosis in both control and Fn-null livers.

Elevated myofibroblast activity in mutant livers.

Myofibroblasts such as activated hepatic stellate cells play a central role in ECM remodeling upon liver injury. Immunofluorescence and Western analysis showed significantly more pronounced expression of α-smooth muscle actin (αSMA), a marker for myofibroblasts in Fn-null livers compared to controls at 17 weeks of CCl_4 treatment ($P < 0.05$; Fig. 2A, B). There was no obvious apoptosis or cell death in either liver type as shown by cleaved caspase 3 immunostaining and no picnotic nuclei with Hoechst 33342 staining at 17 weeks of CCl_4 treatment (Fig. 2C and data not shown).

Significant hepatic dysfunction and increased liver-tissue stiffness in mutant livers.

Next, we examined whether a lack of Fn affects hepatic functions during chronic injury (Fig. 3A-C). Subsequent analyses of serum hepatic biochemical markers (total bilirubin as a measure of hepatic excretory function; cholinesterase and albumin as a measure of hepatic protein synthesis) revealed no apparent differences between control and mutant livers until 8 weeks of CCl_4 treatment. In contrast, in the advanced stage at 17 weeks, mutant mice suffered from a significantly higher level of plasma total bilirubin (0.12 ± 0.02 mg/dl in control [$n = 6$] vs. 0.19 ± 0.04 mg/dl in mutant [$n = 6$], $P = 0.0074$) and lower level of cholinesterase (26.8 ± 1.5 IU/L in control [$n = 6$] vs. 23.4 ± 1.3 IU/L in mutant [$n = 6$], $P = 0.025$). Serum albumin levels were also decreased (3.37 ± 0.10 g/dl in control [$n = 6$] vs. 3.26 ± 0.15 g/dl in mutant [$n = 6$]) but without significance ($P = 0.39$). In addition, liver tissue stiffness as determined by AFM was significantly elevated in Fn-null livers compared to controls at 17 weeks of CCl_4 treatment ($5,128 \pm 553.6$ MPa in mutant vs. $3,313 \pm 835.2$ MPa in control ($n = 9$); $P < 0.05$, Fig. 3D-3G).

Elevated production of latent TGF-β complexes and increased local TGF-β bioavailability in mutant livers.

Fn is associated with latent TGF-β complexes when incorporated into the ECM (16,40) and local TGF-β activity is elevated in Fn-null livers in initial stages following liver injury (26,41). Hence, the effect of Fn-deficiency on the production of latent complexes of TGF-β and local TGF-β bioavailability during advanced chronic liver injury was also investiaged. Pronounced depositions of LAP and of LTBP-1, -3 and -4 in the ECM of mutant livers were shown by immunohistochemistry at 17 weeks of CCl_4 treatment. Interestingly, fibrillar structures were

present even in the absence of Fn (Fig. 4A). Furthermore, the TGF-β activity in mutant livers was significantly higher than in controls at both 8 and 17 weeks of CCl_4 treatment (Fig. 4B, $P < 0.05$), indicating constitutively higher levels of active TGF-β in Fn-null livers during chronic liver injury.

TGF-β promotes the initiation of myofibroblast phenotypes and TGF-β1 alone sufficiently initiates stellate cell activation and transdifferentiation into myofibroblasts after liver injury, whereas Fn extra domain-A (EDA) promotes stellate cell motility but not transdifferentiation into myofibroblasts *in vitro* (26,42). Latent TGF-β that is activated in response to injury binds to the TGF-β type I receptor, which then phosphorylates the C-terminal regions of Smad 2/3 transcription factors. Activated Smads translocate to the nucleus where they are involved in the regulation of gene expression (43,44). Indeed, Fn-null livers showed a significantly increased number of nuclear phospho (p)-Smad2/3-positive nonparenchymal cells ($P < 0.01$) (Fig. 4C). Since constitutively elevated local TGF-β activity was demonstrated in Fn-null livers during chronic liver damage ($P < 0.05$, Fig. 4B), the functional link between TGF-β and myofibroblastic phenotypes at 17 weeks of CCl_4 treatment was further addressed by double immunohistochemical staining. Fn-null livers showed a significantly increased number of p-Smad2/3 and αSMA double-positive myofibroblasts (31.3 ± 5.5 cells/field in mutant; field $= 0.37$ mm² [$n = 10$] vs. 9.8 ± 3.3 cells/field in control [$n = 10$], $P < 0.01$) (Fig. 4D). No nuclear localization of p-Smad2/3 was noted in either non-injured control or Fn-null livers (data now shown).

More disorganized collagen networks with increased lysyl oxidase expressions in mutant livers.

Based on these data, we hypothesized that the collagenous ECM fibrillar network formed in the absence of Fn may differ functionally from Fn-mediated collagenous fibrils, and the more extended fibrosis found in mutant livers (Fig. 1D) was associated with the impaired hepatic functions. Collagen network formation occurs as a multi-step process and contributes to ECM remodeling and maintenance upon tissue damage (45). Therefore, the expression, assembly and degradation levels of the major collagens, type I and III, in the advanced stages of chronic damage was next examined. Highly-disorganized collagen matrices were induced in Fn-null livers. Immunofluorescent observation revealed that extensive networks of type I and III collagen were diffusely distributed in the ECM (Fig.

5A). Type I collagen mRNA levels was also significantly increased in Fn-null livers ($P < 0.05$, Fig. 5B). Collagen networks displayed more disorganized arrangements and significantly larger angular deviation in mutant livers as assessed by Sirius Red stained-samples under the polarized microscope (Fig. 5C-5E). In contrast, control livers formed well-organized, linear type III and type I collagen networks (Fig. 5A, 5C-5E). There were no significant differences in the expression of collagen-related matrix metalloproteinase (MMP) *MMP8* and *MMP13* mRNA levels (Fig. 5F), suggesting that collagen degrading enzymes did not play major roles.

Since type V collagen is an essential element for type III/I collagen fibrillogenesis *in vitro* when Fn is absent (26), the contribution of type V collagen to advanced stages of chronic liver remodeling at 17 weeks of CCl_4 treatment was then determined. Significantly increased deposition and assembly of type V collagen was detected in Fn-null livers in comparison with controls and the localization of assembled fibrils often overlapped with type I collagen fibrils (Fig. 6A). Increased expression of type V collagen mRNA (~1.5-fold) was also observed in mutant livers compared to controls, although the difference was not statistically significant (Fig. 6B). Subsequent ultrastructural analysis using TEM revealed that the mean diameter of collagen fibrils was identical (47.0 ± 9.7 nm in mutant vs. 48.3 ± 8.9 nm in control [$n = 1,500$ fibrils in each]) (Fig. 6C, D). It is known that the diameter of formed type I collagen fibrils is inversely proportional to the type V/type I collagen ratio (46-48). Indeed, a $\sim33\%$ increase in the number of thinner (30-40 nm diameter) and a $\sim21\%$ decrease in the number of thicker (50-60 nm diameter) collagen fibril-subpopulations was found in Fn-null livers compared to controls (Fig. 6D, right panel). Such thinner collagen fibril-subpopulations were also confirmed by AFM analysis (Fig. 3G). Importantly, a significantly increased number of collagen fibrils was demonstrated in mutant livers compared to controls (48.6 ± 7.0 fibrils/ 0.25 μm² in mutant vs. 41.7 ± 4.6 fibrils/ 0.25 μm² in control ($n = 18$); $P < 0.01$, Fig. 6E). The increased fibril number correlated with an increase in hepatic net collagen amount measured by hydroxyproline content ($P < 0.05$, Fig. 6F). Thus, these results indicate that elimination of Fn results in thinner and increased number of collagen fibril organizations/assemblies and suggest both quantitative and qualitative differences between Fn- and type V collagen-mediated type I collagen fibril network formation following tissue injury.

Collagen crosslinking by LOX family members accompanies tissue fibrosis and stiffens tissues (12). Elevated expression of LOX and its subfamily, LOX-like protein (LOXL)2 is detected in both human fibrotic diseases and rodent injury models, and myofibroblasts such as activated hepatic stellate cells are the likely major cellular source of LOX in liver injury (49,50). Since significantly increased liver tissue stiffness alongside the deterioration of net hepatic function was demonstrated in Fn-null livers at 17 weeks of CCl_4 treatment, the functional link between the lack of Fn and LOX expression levels was addressed. LOX and LOXL1-4 mRNA levels were all upregulated in Fn-null livers compared to controls, and LOX was found to be most upregulated in mutant livers (~2.64-fold) compared to controls ($P < 0.01$, Fig. 7A). Therefore, we determined whether elevated TGF-β bioavailability due to absence of Fn is directly involved in the production of LOX in activated hepatic stellate cells *in vitro*. The treatment of Fn-null hepatic stellate cell lines with 2 pM TGF-β1 led to the release of a significant amount of active LOX proteins compared to parental cells (2.46 ± 0.13-fold upregulation in Fn-null vs. 1.60 ± 0.15-fold upregulation in control in response to TGF-β1, $P < 0.01$), whereas no obvious differences in LOX protein levels were observed between them under untreated conditions (Fig. 7B). We further investigated the signaling axis for TGF-β1-mediated LOX expression in Fn-null hepatic stellate cells. Immunocytochemical analysis revealed a significant elevation of LOX expression in Fn-null hepatic stellate cells in response to TGF-β1 (Fig. 7C). Application of Smad3 inhibitor SIS3 following TGF-β1 treatment significantly inhibited (~42.0%) LOX expression in Fn-null hepatic stellate cells. In addition, PI3-kinase inhibitor LY294002 significantly inhibited LOX expression (~38.1%), although to a lesser degree (Fig. 7C). This demonstrates the involvement of both canonical and non-canonical Smad such as PI3 kinase-mediated pathways in TGF-β1-mediated LOX expression in hepatic stellate cells.

Fn-null hepatic stellate cells do not organize type I collagen fibril network in culture, and TGF-β1 can induce type I collagen assembly (26). Therefore, the functional link between TGF-β1-induced LOX and structural and mechanical integrity of collagen fibril network in Fn-null hepatic stellate cells was addressed. Indeed, TGF-β1-induced collagen fibril stiffness in Fn-null hepatic stellate cells was significantly higher compared to control (parental) cells (Fig. 8A, $P < 0.01$). Treatment of Fn-null

stellate cells with 2 pM TGF-β1 and LOX inhibitor β-aminopropionitrile (BAPN, 200 μM) resulted in the disruption of TGF-β-induced fine collagen fibril networks and significantly reduced collagen fibril stiffness ($P < 0.01$) (Fig. 8A, B). Importantly, treatment of Fn-null stellate cells with 10 μg/ml plasma Fn recovered collagen fibril stiffness to control (parental) cell levels (Fig. 8C). Thus, taken together, these findings indicate that elevated TGF-β bioavailability in Fn-null livers induces more active myofibroblasts and sustains their activated phenotypes. As a consequence of this, these myofibroblasts develop more accumulated, disorganized, and LOX-mediated tightly cross-linked collagenous ECMs during advanced chronic liver damage, which thereby results in the significant deterioration of net hepatic function.

Discussion

Our current comprehensive genetic studies with a Fn-deficient animal model provide the following compelling evidence. (1) Elimination of Fn results in elevated local TGF-β activity and continuously increased intracellular TGF-β signaling in activated hepatic stellate cells (myofibroblasts). This results in the development of more advanced liver fibrosis/cirrhosis in Fn-null livers. (2) Fn-null livers exhibit significantly increased LOX expression in chronic liver injury, and Fn-null hepatic stellate cells are a target for the release of active LOX in response to TGF-β1 through both canonical and non-canonical Smad pathways. Thus, we propose that there are the functional links between Fn-mediated control of TGF-β bioavailability and collagen fibril stiffness regulated by LOX. We suggest that such regulatory mechanisms by Fn could be translated for a potential therapeutic target in other chronic fibrotic diseases.

Our current findings in Fn-null mouse livers are consistent with the fact that elevated TGF-β activity induces enhanced differentiation and activation of quiescent fibroblastic cells with a myofibroblastic phenotype (induction of αSMA) in response to tissue damage (5,7). The expression level of αSMA is directly related to the contractile activity of myofibroblasts, which cause tissue contractures (51). This suggests that persistently elevated TGF-β activity due to the lack of Fn induces more highly contractile myofibroblasts and leads to greater ECM secretion accompanied with increased LOX-mediated collagen crosslinking. However, collagen

network reorganization in adult tissues in response to injury is mediated by both Fn and TGF-β-induced type V collagen (26), and our results show both quantitative and qualitative differences between Fn- and type V collagen-mediated type I collagen fibril network formation. Therefore, while the contribution of type V collagen-nucleated collagen fibrogenesis in adult tissues is largely undetermined, our findings support the hypothesis that the accumulation of type V collagen-mediated ECMs during persistent chronic damage has an influence on disorganized ECM 3-dimensional architecture. Such phenotypes occurring beyond the early stages following tissue damage could contribute to the critical turning point from normal to abnormal healing *in vivo*. Consequently, more disorganized and rigid ECMs remarkably impede organ architecture and function. Indeed, accumulating evidence indicates that locally activated TGF-β plays a significant role in the development of liver fibrosis (52-54).

Earlier studies have shown that collagen cross-linking mediated by LOX leads to cancer progression by enhancing ECM receptor integrin signaling (11) and that inhibition of LOX activity partially prevents tissue stiffness following injury (55). Consistent with previous *in vitro* and *in vivo* observations, (11,56,57), our findings indicate that inhibition of collagen cross linking by BAPN affects TGF-β-induced structural and mechanical integrity of collagenous ECM networks in Fn-null hepatic stellate cells. We have demonstrated functional links between tissue/organ functions and regulatory mechanisms of LOX underlying chronic fibrotic disease such as liver fibrosis/cirrhosis. Bone morphogenic protein 1 (BMP 1), an extracellular metalloproteinase, and periostin, a secretory protein in connective tissues, are major activators of LOX and interact with Fn (58,59). Fn-null embryonic fibroblasts dramatically decrease proteolytic processing of the 45 kDa LOX proenzyme to the 32 kDa active form without changing BMP1 levels compared to control cells, suggesting the regulatory role of Fn matrix in LOX catalytic activity (60). In contrast, we have shown that Fn-null hepatic stellate cells release significant amount of active LOX in response to TGF-β1 without Fn matrix. Interestingly, this TGF-β1-LOX signaling axis in Fn-null hepatic stellate cells is mediated through both canonical and non-canonical pathways (61). A very recent observation has documented that the expression level of periostin is significantly upregulated in both acute and chronic liver injury, and TGF-β1 can induce periostin in hepatic stellate cells *in vitro* (62). Thus, periostin is likely to be involved in TGF-β1-induced LOX activation in Fn-null hepatic stellate cells as cell type specific phenotyptes.

Little insight into the pathophysiological roles of Fn has emerged from studies of genetic changes in humans. There are no documented cases of Fn-null patients, the nearest condition being familial glomerulonephritis in which there are mutations in the type III modules of Fn (63). Whilst complete Fn-null mice show an embryonic lethal phenotype (64), experimental evidence has documented that skin wounds heal normally in mice lacking plasma type Fn (30), hence an absolute requirement for Fn in response to adult tissue damage has been speculative. The current findings imply that Fn regulates the balance between active and inactive (latent) TGF-β, which in turn modulates ECM production and remodeling following injury, and consequently retains adult tissue/organ functions. A number of genetic studies suggest that the absence of, or a mutation in, LLC-binding ECMs such as fibrillin-1 and -2 results in increased TGF-β activity and Smad signaling, whereas the absence of, or mutation in, LTBPs results in decreased activity and signaling (65-70). We have demonstrated that the absence of Fn results in increased TGF-β bioavailability following organ injury. A possible explanation for elevated TGF-β bioavailability is that the deficiency of LLC-binding ECMs, as seen in this Fn-null model, decreases the matrix sequestration of LLCs, which thereby renders latent TGF-β more accessible for activation with negative consequences for cellular functions (71). In contrast, there were very limited *in vivo* observations for negative regulation of TGF-β bioavailability by Fn. A recent study reveals that the inhibition of cell-mediated Fn matrix assembly without affecting its production by peptide pUR4 shows the normal release of active TGF-β in hepatic stellate cells *in vitro* (72). However, Fn matrix networks play crucial roles in many important biological events and in adult homeostasis (21,22). Fn matrix networks promote parenchymal cell survival such as hepatocytes following liver damage (23), and the elimination of Fn extradomain-A (EDA) splicing domain results in a shorter life span (73). Therefore, the regulation of TGF-β bioavailability by Fn with retaining Fn matrix networks would be essential elements for long-term anti-fibrotic strategies in chronic fibrotic diseases to preserve tissue/organ function and homeostasis.

Conflict of interest
The authors disclose no conflicts.

Author contributions
Takao Sakai conceived ideas, designed experiments, and supervised the project. Ayumi Iwasaki, Keiko Sakai, Kei Moriya, Takayoshi Miyazono, and Satoshi Yasumura performed experiments. Douglas Keene carried out transmission electron microscopy studies, and Riaz Akhtar carried out atomic force microscopy studies. Takako Sasaki generated anti-type I, III and V collagen, LAP, LTBP-3 and 4, and LOX antibodies. Ayumi Iwasaki, Keiko Sakai, Kei Moriya, Riaz Akhtar, Takayoshi Miyazono, Satoshi Yasumura, Masatoshi Watanabe, Shin Morishita, and Takao Sakai analyzed the data. Takao Sakai wrote and edited the manuscript.

References

1.   Diehl, A. M., and Chute, J. (2013) Underlying potential: cellular and molecular determinants of adult liver repair. *The Journal of clinical investigation* **123**, 1858-1860

2.   Bataller, R., and Brenner, D. A. (2005) Liver fibrosis. *The Journal of clinical investigation* **115**, 209-218

3.   Friedman, S. L. (2010) Evolving challenges in hepatic fibrosis. *Nat Rev Gastroenterol Hepatol* **7**, 425-436

4.   Schuppan, D., and Kim, Y. O. (2013) Evolving therapies for liver fibrosis. *The Journal of clinical investigation* **123**, 1887-1901

5.   Wallace, K., Burt, A. D., and Wright, M. C. (2008) Liver fibrosis. *Biochem J* **411**, 1-18

6.   Forbes, S. J., and Parola, M. (2011) Liver fibrogenic cells. *Best practice & research. Clinical gastroenterology* **25**, 207-217

7.   Hinz, B., Phan, S. H., Thannickal, V. J., Galli, A., Bochaton-Piallat, M. L., and Gabbiani, G. (2007) The myofibroblast: one function, multiple origins. *The American journal of pathology* **170**, 1807-1816

8.   Kolacna, L., Bakesova, J., Varga, F., Kostakova, E., Planka, L., Necas, A., Lukas, D., Amler, E., and Pelouch, V. (2007) Biochemical and biophysical aspects of collagen nanostructure in the extracellular matrix. *Physiological research / Academia Scientiarum Bohemoslovaca* **56 Suppl 1**, S51-60

9.   Lucero, H. A., and Kagan, H. M. (2006) Lysyl oxidase: an oxidative enzyme and effector of cell function. *Cell Mol Life Sci* **63**, 2304-2316

10.   Csiszar, K. (2001) Lysyl oxidases: a novel multifunctional amine oxidase family. *Prog Nucleic Acid Res Mol Biol* **70**, 1-32

11.   Levental, K. R., Yu, H., Kass, L., Lakins, J. N., Egeblad, M., Erler, J. T., Fong, S. F., Csiszar, K., Giaccia, A., Weninger, W., Yamauchi, M., Gasser, D. L., and Weaver, V. M. (2009) Matrix crosslinking forces tumor progression by enhancing integrin signaling. *Cell* **139**, 891-906

12.   van der Slot, A. J., van Dura, E. A., de Wit, E. C., De Groot, J., Huizinga, T. W., Bank, R. A., and Zuurmond, A. M. (2005) Elevated formation of pyridinoline cross-links by profibrotic cytokines is associated with enhanced lysyl hydroxylase 2b levels. *Biochim Biophys Acta* **1741**, 95-102

13.   Gressner, A. M., Weiskirchen, R., Breitkopf, K., and Dooley, S. (2002) Roles of TGF-beta in hepatic fibrosis. *Front Biosci* **7**, d793-807

14.   Hayashi, H., and Sakai, T. (2012) Biological Significance of Local TGF-beta Activation in Liver Diseases. *Frontiers in physiology* **3**, 12

15.   Dallas, S. L., Sivakumar, P., Jones, C. J., Chen, Q., Peters, D. M., Mosher, D. F., Humphries, M. J., and Kielty, C. M. (2005) Fibronectin regulates latent transforming growth factor-beta (TGF beta) by controlling matrix assembly of latent TGF beta-binding protein-1. *The Journal of biological chemistry* **280**, 18871-18880

16.   Rifkin, D. B. (2005) Latent transforming growth factor-beta (TGF-beta) binding proteins: orchestrators of TGF-beta availability. *The Journal of biological chemistry* **280**, 7409-7412

17.   Margadant, C., and Sonnenberg, A. (2010) Integrin-TGF-beta crosstalk in fibrosis, cancer and wound healing. *EMBO Rep* **11**, 97-105

18.   Sheppard, D. (2006) Transforming growth factor beta: a central modulator of pulmonary and airway inflammation and fibrosis. *Proc Am Thorac Soc* **3**, 413-417

19.   Varga, J., and Pasche, B. (2009) Transforming growth factor beta as a therapeutic target in systemic sclerosis. *Nat Rev Rheumatol* **5**, 200-206

20.   Nishimura, S. L. (2009) Integrin-mediated transforming growth factor-beta activation, a potential therapeutic target in fibrogenic disorders. *The American journal of pathology* **175**, 1362-1370

21.   Hynes, R. O. (1990) *Fibronectins*, Springer-Verlag, New York

22.   Mosher, D. F. (1989) *Fibronectin*, Academic Press, San Diego

23.   Moriya, K., Sakai, K., Yan, M. H., and Sakai, T. (2012) Fibronectin is essential for survival but is dispensable for proliferation of hepatocytes in acute liver injury in mice. *Hepatology (Baltimore, Md.)* **56**, 311-321

24.   Velling, T., Risteli, J., Wennerberg, K., Mosher, D. F., and Johansson, S. (2002) Polymerization of type I and III collagens is dependent on fibronectin and enhanced by integrins alpha 11beta 1 and alpha 2beta 1. *The Journal of biological chemistry* **277**, 37377-37381

25. Sottile, J., Shi, F., Rublyevska, I., Chiang, H. Y., Lust, J., and Chandler, J. (2007) Fibronectin-dependent collagen I deposition modulates the cell response to fibronectin. *Am J Physiol Cell Physiol* **293**, C1934-1946

26. Moriya, K., Bae, E., Honda, K., Sakai, K., Sakaguchi, T., Tsujimoto, I., Kamisoyama, H., Keene, D. R., Sasaki, T., and Sakai, T. (2011) A fibronectin-independent mechanism of collagen fibrillogenesis in adult liver remodeling. *Gastroenterology* **140**, 1653-1663

27. Constandinou, C., Henderson, N., and Iredale, J. P. (2005) Modeling liver fibrosis in rodents. *Methods Mol Med* **117**, 237-250

28. Nowack, H., Gay, S., Wick, G., Becker, U., and Timpl, R. (1976) Preparation and use in immunohistology of antibodies specific for type I and type III collagen and procollagen. *J Immunol Methods* **12**, 117-124

29. Timpl, R. (1982) Antibodies to collagens and procollagens. *Methods in enzymology* **82 Pt A**, 472-498

30. Sakai, T., Johnson, K. J., Murozono, M., Sakai, K., Magnuson, M. A., Wieloch, T., Cronberg, T., Isshiki, A., Erickson, H. P., and Fassler, R. (2001) Plasma fibronectin supports neuronal survival and reduces brain injury following transient focal cerebral ischemia but is not essential for skin-wound healing and hemostasis. *Nat Med* **7**, 324-330

31. Sakai, T., Li, S., Docheva, D., Grashoff, C., Sakai, K., Kostka, G., Braun, A., Pfeifer, A., Yurchenco, P. D., and Fassler, R. (2003) Integrin-linked kinase (ILK) is required for polarizing the epiblast, cell adhesion, and controlling actin accumulation. *Genes Dev* **17**, 926-940

32. Maeda, T., Sakabe, T., Sunaga, A., Sakai, K., Rivera, A. L., Keene, D. R., Sasaki, T., Stavnezer, E., Iannotti, J., Schweitzer, R., Ilic, D., Baskaran, H., and Sakai, T. (2011) Conversion of mechanical force into TGF-beta-mediated biochemical signals. *Curr Biol* **21**, 933-941

33. Whittaker, P., and Przyklenk, K. (2009) Fibrin architecture in clots: a quantitative polarized light microscopy analysis. *Blood Cells Mol Dis* **42**, 51-56

34. Katoh, K., Hammar, K., Smith, P. J., and Oldenbourg, R. (1999) Arrangement of radial actin bundles in the growth cone of Aplysia bag cell neurons shows the immediate past history of filopodial behavior. *Proc Natl Acad Sci U S A* **96**, 7928-7931

35. Madibally, S. V., Solomon, V., Mitchell, R. N., Van De Water, L., Yarmush, M. L., and Toner, M. (2003) Influence of insulin therapy on burn wound healing in rats. *J Surg Res* **109**, 92-100

36. Papi, M., Paoletti, P., Geraghty, B., and Akhtar, R. (2014) Nanoscale characterization of the biomechanical properties of collagen fibrils in the sclera. *Applied Physics Letters* **104**, 103703

37. Honda, K., Sakaguchi, T., Sakai, K., Schmedt, C., Ramirez, A., Jorcano, J. L., Tarakhovsky, A., Kamisoyama, H., and Sakai, T. (2007) Epidermal hyperplasia and papillomatosis in mice with a keratinocyte-restricted deletion of csk. *Carcinogenesis* **28**, 2074-2081

38. Abe, M., Harpel, J. G., Metz, C. N., Nunes, I., Loskutoff, D. J., and Rifkin, D. B. (1994) An assay for transforming growth factor-beta using cells transfected with a plasminogen activator inhibitor-1 promoter-luciferase construct. *Anal Biochem* **216**, 276-284

39. Schuppan, D., and Afdhal, N. H. (2008) Liver cirrhosis. *Lancet* **371**, 838-851

40. Hynes, R. O. (2009) The extracellular matrix: not just pretty fibrils. *Science* **326**, 1216-1219

41. Kawelke, N., Vasel, M., Sens, C., Au, A., Dooley, S., and Nakchbandi, I. A. (2011) Fibronectin protects from excessive liver fibrosis by modulating the availability of and responsiveness of stellate cells to active TGF-beta. *PLoS One* **6**, e28181

42. Olsen, A. L., Sackey, B. K., Marcinkiewicz, C., Boettiger, D., and Wells, R. G. (2012) Fibronectin extra domain-A promotes hepatic stellate cell motility but not differentiation into myofibroblasts. *Gastroenterology* **142**, 928-937 e923

43. Massague, J., Seoane, J., and Wotton, D. (2005) Smad transcription factors. *Genes Dev* **19**, 2783-2810

44. Moustakas, A., and Heldin, C. H. (2009) The regulation of TGFbeta signal transduction. *Development* **136**, 3699-3714

45. Canty, E. G., and Kadler, K. E. (2005) Procollagen trafficking, processing and fibrillogenesis. *Journal of cell science* **118**, 1341-1353

46. Adachi, E., and Hayashi, T. (1986) In vitro formation of hybrid fibrils of type V collagen and type I collagen. Limited growth of type I collagen into thick fibrils by type V collagen. *Connect Tissue Res* **14**, 257-266

47. Wenstrup, R. J., Florer, J. B., Brunskill, E. W., Bell, S. M., Chervoneva, I., and Birk, D. E. (2004) Type V collagen controls the initiation of collagen fibril assembly. *The Journal of biological chemistry* **279**, 53331-53337

48. Birk, D. E. (2001) Type V collagen: heterotypic type I/V collagen interactions in the regulation of fibril assembly. *Micron* **32**, 223-237

49. Perepelyuk, M., Terajima, M., Wang, A. Y., Georges, P. C., Janmey, P. A., Yamauchi, M., and Wells, R. G. (2013) Hepatic stellate cells and portal fibroblasts are the major cellular sources of collagens and lysyl oxidases in normal liver and early after injury. *Am J Physiol Gastrointest Liver Physiol* **304**, G605-614

50. Barry-Hamilton, V., Spangler, R., Marshall, D., McCauley, S., Rodriguez, H. M., Oyasu, M., Mikels, A., Vaysberg, M., Ghermazien, H., Wai, C., Garcia, C. A., Velayo, A. C., Jorgensen, B., Biermann, D., Tsai, D., Green, J., Zaffryar-Eilot, S., Holzer, A., Ogg, S., Thai, D., Neufeld, G., Van Vlasselaer, P., and Smith, V. (2010) Allosteric inhibition of lysyl oxidase-like-2 impedes the development of a pathologic microenvironment. *Nat Med* **16**, 1009-1017

51. Guyot, C., Lepreux, S., Combe, C., Doudnikoff, E., Bioulac-Sage, P., Balabaud, C., and Desmouliere, A. (2006) Hepatic fibrosis and cirrhosis: the (myo)fibroblastic cell subpopulations involved. *Int J Biochem Cell Biol* **38**, 135-151

52. Kondou, H., Mushiake, S., Etani, Y., Miyoshi, Y., Michigami, T., and Ozono, K. (2003) A blocking peptide for transforming growth factor-beta1 activation prevents hepatic fibrosis in vivo. *Journal of hepatology* **39**, 742-748

53. Drews, F., Knobel, S., Moser, M., Muhlack, K. G., Mohren, S., Stoll, C., Bosio, A., Gressner, A. M., and Weiskirchen, R. (2008) Disruption of the latent transforming growth factor-beta binding protein-1 gene causes alteration in facial structure and influences TGF-beta bioavailability. *Biochim Biophys Acta* **1783**, 34-48

54. Wang, B., Dolinski, B. M., Kikuchi, N., Leone, D. R., Peters, M. G., Weinreb, P. H., Violette, S. M., and Bissell, D. M. (2007) Role of alphavbeta6 integrin in acute biliary fibrosis. *Hepatology (Baltimore, Md.)* **46**, 1404-1412

55. Georges, P. C., Hui, J. J., Gombos, Z., McCormick, M. E., Wang, A. Y., Uemura, M., Mick, R., Janmey, P. A., Furth, E. E., and Wells, R. G. (2007) Increased stiffness of the rat liver precedes matrix deposition: implications for fibrosis. *Am J Physiol Gastrointest Liver Physiol* **293**, G1147-1154

56. Zhao, R., Chen, C. S., and Reich, D. H. (2014) Force-driven evolution of mesoscale structure in engineered 3D microtissues and the modulation of tissue stiffening. *Biomaterials* **35**, 5056-5064

57. Mammoto, A., Mammoto, T., Kanapathipillai, M., Wing Yung, C., Jiang, E., Jiang, A., Lofgren, K., Gee, E. P., and Ingber, D. E. (2013) Control of lung vascular permeability and endotoxin-induced pulmonary oedema by changes in extracellular matrix mechanics. *Nature communications* **4**, 1759

58. Huang, G., Zhang, Y., Kim, B., Ge, G., Annis, D. S., Mosher, D. F., and Greenspan, D. S. (2009) Fibronectin binds and enhances the activity of bone morphogenetic protein 1. *The Journal of biological chemistry* **284**, 25879-25888

59. Maruhashi, T., Kii, I., Saito, M., and Kudo, A. (2010) Interaction between periostin and BMP-1 promotes proteolytic activation of lysyl oxidase. *The Journal of biological chemistry* **285**, 13294-13303

60. Fogelgren, B., Polgar, N., Szauter, K. M., Ujfaludi, Z., Laczko, R., Fong, K. S., and Csiszar, K. (2005) Cellular fibronectin binds to lysyl oxidase with high affinity and is critical for its proteolytic activation. *The Journal of biological chemistry* **280**, 24690-24697

61. Voloshenyuk, T. G., Landesman, E. S., Khoutorova, E., Hart, A. D., and Gardner, J. D. (2011) Induction of cardiac fibroblast lysyl oxidase by TGF-beta1 requires PI3K/Akt, Smad3, and MAPK signaling. *Cytokine* **55**, 90-97

62. Huang, Y., Liu, W., Xiao, H., Maitikabili, A., Lin, Q., Wu, T., Huang, Z., Liu, F., Luo, Q., and Ouyang, G. (2015) Matricellular protein periostin contributes to hepatic inflammation and fibrosis. *The American journal of pathology* **185**, 786-797

63. Castelletti, F., Donadelli, R., Banterla, F., Hildebrandt, F., Zipfel, P. F., Bresin, E., Otto, E., Skerka, C., Renieri, A., Todeschini, M., Caprioli, J., Caruso, R. M., Artuso, R., Remuzzi, G., and Noris, M. (2008) Mutations in FN1 cause glomerulopathy with fibronectin deposits. *Proc Natl Acad Sci U S A* **105**, 2538-2543